Toxicology Mechanisms and Methods, 2011; 21(8): 606–621
© 2011 Informa Healthcare USA, Inc.
ISSN 1537-6516 print/ISSN 1537-6524 online
DOI: 10.3109/15376516.2011.572934

informa
healthcare

RESEARCH ARTICLE

ESI-Mass spectrometric and HPLC elucidation of a new ergot alkaloid from perennial ryegrass hay silage associated with bovine reproductive problems

Andreas F. Lehner[1], Jennifer M. Duringer[2], Charles T. Estill[3], Thomas Tobin[4], and A. Morrie Craig[5]

[1]Michigan State University, Diagnostic Center for Population & Animal Health, Lansing, Michigan 48910, USA, [2]Oregon State University, Department of Environmental & Molecular Toxicology, Corvallis Oregon 97331, USA, [3]Oregon State University, Department of Clinical Sciences, College of Veterinary Medicine, Corvallis Oregon 97331, USA, [4]University of Kentucky, Department of Veterinary Science, Maxwell H. Gluck Equine Research Center, Lexington Kentucky 40546, USA, and [5]Oregon State University, Department of Biomedical Sciences, College of Veterinary Medicine, Corvallis Oregon 97331, USA

Abstract

This case report involves four dairies in the Willamette Valley, Oregon, which experienced reproductive problems associated with the presence of a large, previously unidentified, peak eluting at 5 min in a standard ergovaline high-performance liquid chromatography assay of perennial ryegrass silage fed to those animals. Mycotoxin analysis of the silage was negative, as was serological screening of the herds for infectious bovine rhinotracheitis, bovine diarrhea virus and *Leptospirosis*, including culturing of urine for *Leptospira hardjo hardjobovis*. Prolactin concentrations were low in most cattle, consistent with ingestion of ergot alkaloids. We believe that this peak represents a novel ergot alkaloid-related compound due to its extractability with Ergosil, its detectability due to fluorescence, and its chromatographic retention between ergovaline (mw = 533) and ergotamine (mw = 581). Its molecular weight was calculated as 570 owing to the predominance of a *m/z* 593.5 ion in the full scan ESI(+)MS and its deduced tendency to complex with Na^+ (as *m/z* 593) or K^+ (as *m/z* 609) ions. We offer rationales for elucidation of the structure of this compound, with the closest starting point comprising an m.w. of 566—a fructofuranosyl-(2-1)-O-beta-D-fructofuranoside derivative of 6,7-secoergoline from *Claviceps fusiformis*. This m.w. requires modifications, such as reduction of two double bonds in the secoergoline component to give the target 570 m.w. Despite the lack of a definitive structure, the analysis herein provides a starting point for eventual elucidation of this apparently new ergot alkaloid, and to guide and encourage further investigation as to its association with endophyte toxicosis in livestock.

Keywords: Ergot alkaloids, silage, ryegrass, dairy cows, reproductive problems

Introduction

Perennial ryegrass (*Lolium perenne*) is a cool-season grass which is infected with the endophytic fungus *Neotyphodium lolii*. This symbiotic endophyte infection confers benefits to the plant such as insect resistance, growth enhancement and drought tolerance (Joost, 1995), thereby decreasing the need for pesticides, fertilizers and irrigation. The fungus provides some of these benefits through production of insect-repelling alkaloids, particularly peramine; other compounds are also synthesized, including lolitrem and ergot alkaloids (Cheeke, 1998). Unfortunately, cattle and other herbivores that ingest these alkaloids experience deleterious effects, which have been grouped under the umbrella term "endophyte toxicosis," when endophyte-infected grasses are grazed or fed as hay/silage (Oliver, 2005). The alkaloid lolitrem B is responsible for the neurological syndrome known as "ryegrass staggers" which involves a reversible tremoring response in the skeletal musculature of affected animals due to inhibition of large

Address for Correspondence: Dr. Andreas Lehner, Diagnostic Center for Population and Animal Health, Michigan State University, 4125 Beaumont Road, Lansing, MI 48910-8104, USA. Tel.: 1-517-432-5866; Fax: 517-353-9080. E-mail: LehnerA@dcpah.msu.edu

(Received 28 January 2011; revised 10 March 2011; accepted 13 March 2011)

conductance calcium-activated potassium channels (Dalziel et al., 2005). Toxicological effects due to ingestion of ergot alkaloids are much broader in scope and include vasoconstriction in the extremities, decreased weight gain, a decrease or loss in milk production and lower reproductive efficiency (Oliver, 1997), all of which result in a $1 billion loss to livestock producers annually in the United States (Browning, 2004).

Ergot alkaloids are agonists of dopamine D_2 receptors and, as such, inhibit prolactin secretion, resulting in reduced milk yield and quality (Brown et al., 1996; Lean, 2001; Kim et al., 2007) and decreased mammary development (Porter & Thompson, 1992; Blodgett, 2001). Since decreased serum prolactin concentration is one of the more consistent findings in livestock feeding studies involving endophyte-infected forage, it is often used as a diagnostic indicator of endophyte toxicosis. The action of ergot alkaloids as alpha-2 adrenergic agonists results in vasoconstriction of blood vessels which may further influence milk production by decreasing blood flow to the mammary gland and splanchnic bed (Lean, 2001). Additionally, lower concentrations of luteinizing hormone and prostaglandins (Browning et al., 1998) and altered corpus luteum development (Porter & Thompson, 1992; Burke et al., 2001) have been noted in animals exposed to ergot alkaloids. These effects generally result in difficulty maintaining pregnancy which manifests as lowered reproductive efficiency in cattle herds.

Few reports have directly examined the effects of endophyte-infected hay silage on livestock production, but preliminary evidence indicates that the ensiling process does not significantly alter the concentration of ergot alkaloids in endophyte-infected forage (Roberts et al., 2002). Physiological effects associated with endophyte toxicosis have been previously observed in dairy cattle fed ensiled, endophyte-infected hay (Jackson et al., 1988; Lean, 2001).

Our case report involves four dairies in the Willamette Valley, Oregon, which experienced reproductive problems from 2003 to 2005. The rural practice veterinarian and a toxicologist from Oregon State University, College of Veterinary Medicine, which were working on these cases, met jointly with the owners of the four dairies. They discovered that the affected cattle had common symptomologies, including reduced conception rates, increased incidence of abortions, lower than expected milk production and reduced serum prolactin levels in breeding animals, clinical signs consistent with ergot alkaloid toxicity. A screening of feed for typical ergot alkaloids associated with endophyte toxicosis was negative; however, all samples analyzed provided evidence of a previously unseen compound eluting as a single prominent chromatographic peak at 5 min in an ergovaline high-performance liquid chromatography (HPLC) assay (Craig et al., 1994) from perennial ryegrass silage fed to these animals. The objective of this study is to present the clinical findings from these herds and to characterize the new peak using mass spectroscopy to reveal clues about its chemical structure and identity.

Materials and methods

Description and clinical evaluation of dairy herds

Four dairy herds that ranged from 50 to 1950 milking head in a 50-mile radius of Corvallis, Oregon, began experiencing a reduction in fertility during the summer of 2003. Specifically, these herds showed a lack of display of estrus, decreased uterine tone at the time of breeding, decreased conception rate and an increase in early embryonic death.

Mycotoxin analysis (a screening assay for vomitoxin, aflatoxins, zearalenone, T-2 toxin and fumonisin) of silage samples collected from the dairies at the onset of fertility problems was performed via HP-TLC or ELISA by Dr. Lloyd Bennett of the Mississippi State University Veterinary Diagnostic Laboratory. Serological screening for infectious bovine rhinotracheitis (Rossi & Kiesel, 1971; Cottral, 1978), bovine diarrhea virus (Rossi & Kiesel, 1971; Cottral, 1978) and *Leptospirosis* (Cole et al., 1973) and culturing of urine for *Leptospira hardjo hardjobovis* (National Veterinary Services Laboratories, 2001) was carried out on samples from two herds at the Veterinary Diagnostic Laboratory, Oregon State University. These tests were conducted to rule out common causes of infectious infertility. Blood was also sampled from three of the four herds and analyzed for prolactin concentration via radioimmunoassay (Bernard et al., 1993) by Dr. Neil Schrick of the University of Tennessee, Department of Animal Science.

Collection and preparation of hay and silage samples

Approximately, 50 silage samples were collected over multiple days from each of the four herds at the time fertility problems were identified and on a monthly basis for approximately 4 months following. Samples were dried in a chemical hood at room temperature over 2–5 days until they were judged to be dry and were submitted to the Endophyte Service Laboratory, Oregon State University, for ergovaline analysis. Dried samples were ground to a fine consistency that enabled them to pass through a 0.5-mm screen (Cyclotec 1093 sample mill, Tecator, Hönganäs, Sweden).

Ergovaline HPLC analysis and collection of new peak

Ergovaline concentration was analyzed according to a previously reported method (Craig et al., 1994). Briefly, ergotamine tartrate (internal standard) was added to 1.0 g of ground sample which was then extracted with chloroform and sodium hydroxide by turning in the dark over 24 h. Next, the sample was centrifuged at 2000 rpm for 5 min. Solid phase extraction columns containing Ergosil (Analtech, Newark, DE) were conditioned with chloroform before the sample supernatant was applied and drawn through the column. The column was then

© 2011 Informa Healthcare USA, Inc.

washed with a chloroform:acetone mixture followed by methanol. The ergot alkaloids were eluted with methanol and concentrated by nitrogen evaporation before analysis by HPLC. A polymeric divinyl benzene column (Jordi RP SM-500A, 5µ (150 mm × 4.6 mm)) was employed with a mobile phase of acetonitrile/2.5 mM ammonium carbonate (70/30 v/v) and run at a flow of 1.0 mL/min. Detection was by fluorescence with excitation and emission wavelengths of 250 and 420 nm, respectively.

A new peak, eluting at approximately 5 min in the ergovaline HPLC assay, appeared in perennial ryegrass silage samples at varying concentrations (Figure 1). To concentrate and purify this peak, samples with a large concentration of this compound were extracted using the ergovaline methodology, pooled, dried under a nitrogen stream at 50°C and reconstituted in 0.5 mL methanol. The pooled sample was then vortexed, sonicated and centrifuged for 5 min at 2000 rpm. The supernatant was injected onto the HPLC system and the peak eluting at 5 min was captured by manual fraction collection. The corresponding fraction was dried under a nitrogen stream at 50°C, reconstituted with 1 mL methanol, vortexed, sonicated and centrifuged for 5 min at 2000 rpm. The final supernatant was stored in an amber vial in the freezer (–20°C) until mass spectral analysis was performed.

ESI(+)-ion trap mass spectrometry

Spectra were first obtained on a LCQ Classic ion trap mass spectrometer (Thermo Finnigan, Waltham, MA) equipped with a custom-designed electrospray inlet consisting of a 30 micron i.d. steel capillary heated at 170°C and operated at 2.7 kV. Solvent flow was controlled by a HPLC system consisting of a Waters (Milford, MA) Automated Gradient Controller with two Waters 515 HPLC pumps and a Rheodyne 8125 injector. The HPLC solvents used were water and acetonitrile, each containing 0.1% acetic acid and 0.01% trifluoroacetic acid eluting under isocratic conditions in a 50:50 ratio. Samples were introduced to the spectrometer by loop injection with data acquisition in the positive ion mode. MS/MS analysis was performed on MS peaks with the highest relative intensity.

ESI(+)MS/MS

A Micromass Quattro II ESI(+)-MS/MS (Beverly, MA) was calibrated with polyethylene glycol 400 standard and tuned for positive ion mass spectrometry by direct

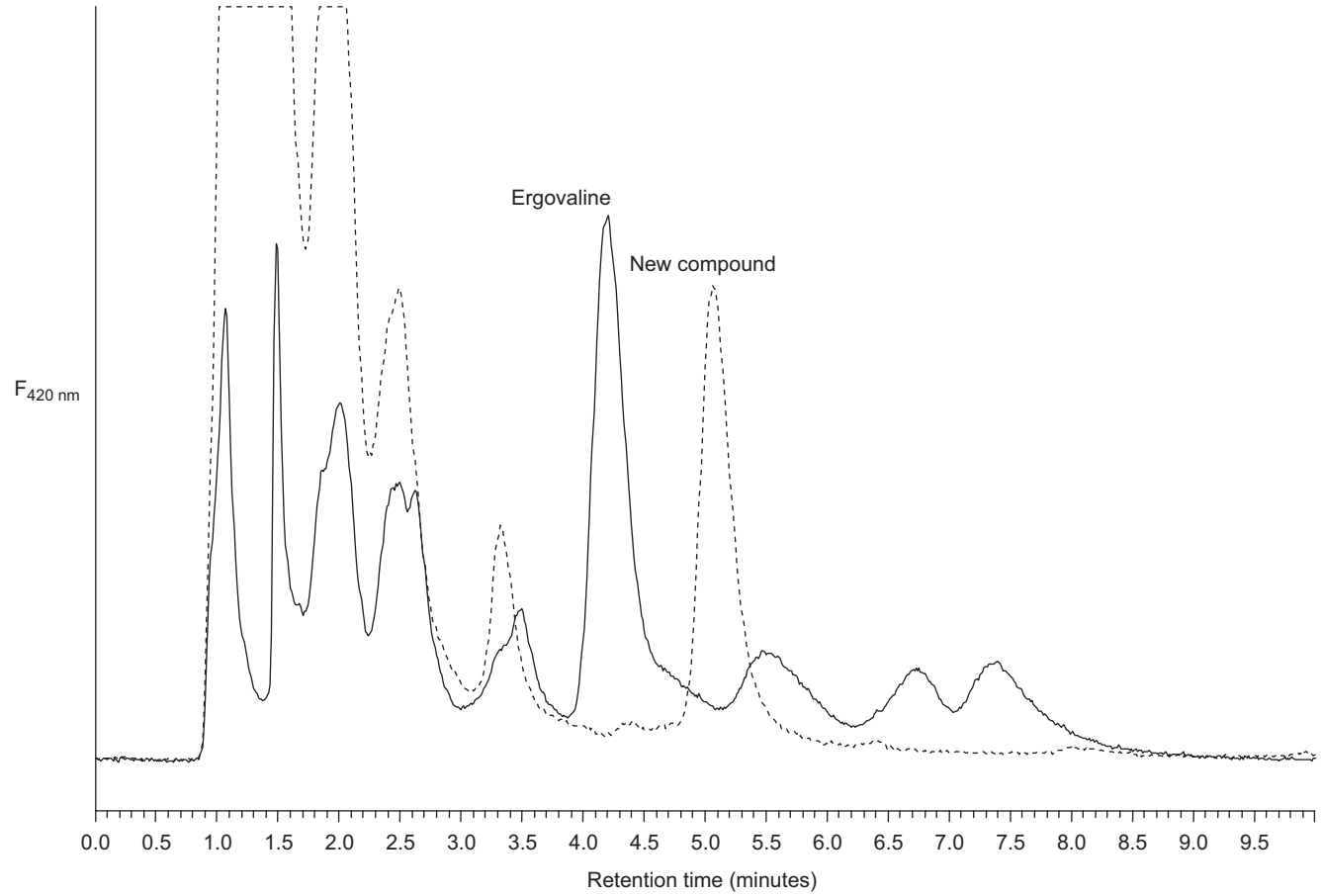

Figure 1. HPLC chromatogram of an extract of fescue straw control (dark solid line) overlaid with that of a silage sample containing the new peak at 5 min (gray dotted line). Ergovaline elutes at 4.1-min retention time, and ergotamine standard (data not shown) at 6.1-min retention time; the unknown peak under investigation elutes at 5.1-min retention time. The y-axis shows relative fluorescence emission at 420 nm following excitation at 250 nm.

infusion of 10 μg/mL ergocryptine (Sigma) in 0.05% formic acid (aq):acetonitrile, 1:1 at 25 μL/min. The peak shape and intensity of the ergocryptine *m/z* 576 monoprotonated [M + H] ion was optimized by adjustment of capillary, HV lens, cone voltage, skimmer lens and RF lens settings. Skimmer lens offset was 5 V. Collision gas (argon) and collision energy were adjusted for collision-induced dissociation in the central hexapole by optimization of settings as needed for the second quadrupole. Generally, the collision gas was set to ~2×10^{-3} mbar. The photomultiplier was set at 750–800 V for maximum sensitivity. A cone voltage setting of 38 and a collision energy setting of 37.5 provided optimal generation of daughter ions, particularly *m/z* 223 and 208, from the ergocryptine *m/z* 576 ion.

Formula calculator

Molecular formulae were calculated by a downloadable program called Formula Calculator JMB3, version 3.9, written by John M. Bland, Ph.D., of the USDA, ARS, SRRC, New Orleans, LA, and available at www.ars.usda.gov/services by clicking on "Software." Formulae were calculated for a 570 ± 0.5 molecular weight by assuming it was in the range C_{10-40} H_{0-97} O_{1-15} N_{1-15} S_{0-1} with a possible maximum unsaturation (double bonds plus rings) of 15.

Relative abundance

Relative abundance of M+1 and M+2 isotope peaks in derived molecular formulae were calculated in percentage units as follows in a Microsoft Excel 2007 spreadsheet:

1.[M+1] = (1.108 × C) + (0.365 × N) + (0.037 × O) + (0.015 × H) + (0.79 × S) and

2.[M+2] = ((1.108 × C)²/200) + (0.204 × O) + ((0.015 × H)²/200 + ((0.365 × N)^2/200) + (4.43 × S)

where C = # carbons, N = # nitrogens, O = # oxygens, S = # sulfurs and H = # hydrogens. The resultant calculated isotopic abundances, particularly M+2 values, gave values close to those derived with available software packages including Mass Spec Calculator and Isoform (see below).

Mass spectrometric calculations

Candidate structures, their fragmentations and isotopic relative abundances, and the relative abundances of various molecular formulae were assessed and verified by the assistance of Mass Spec Calculator Professional, version 4.03 software (Quadtech Associates, Inc., 1998, published by ChemSW, Inc., Fairfield, CA), and Isoform version 1.02 (1997) from the National Institute of Standards and Tehnology (NIST), Gaithersburg, MD. Mass spectral libraries were searched with Wiley 7th Edition Mass Spectral Browser (Palisade Corporation, Newfield, NY) and Agilent Enhanced Chemstation (Santa Clara, CA) software.

Merck Index search

Molecular weight searches were carried out with ChemFinder software, version 7.0m, available from CambridgeSoft (Cambridge, MA), associated with the Merck Index, 13th Edition (2001).

Results

Clinical evaluation

Microbiological and toxicological assays were negative. Mycotoxin analysis revealed no mycotoxins present at concentrations normally associated with clinical disease in cattle. Blood and urine screens for the viral and bacterial pathogens listed previously were negative. In agreement with a history of reproductive problems (an inability to conceive, abortions, low milk production), prolactin concentrations were low for all animals except for a small group of isolated heifers from one dairy. Taken together, clinical signs were generally consistent with and suggestive of endophyte toxicosis.

Mass spectral analysis of the new peak

Perennial ryegrass silage extracted and examined according to validated methods worked out for ergot alkaloids revealed a unique peak at ~5.0 min retention time (RT) (Figure 1). This RT is in a unique chromatographic zone between the elution times for ergovaline (shown in Figure 1) and ergotamine (data not shown) in which very few ergot alkaloids have been identified. Full scan ESI(+)-ion trap mass spectrometry of concentrated fractions of the ~5.0 min RT peak is shown in Figure 2, indicating a principal peak at *m/z* 593.5 with associated isotopic abundances at M+1 = 37.3%, M+2 = 9.4% and M+3 = 1.6%. Additional minor peaks were visible at *m/z* 282, 463, 507, 535, 551, 611 and 639.

MS^n ion trap mass spectrometry revealed product ion spectra as shown in Figure 3. *M/z* 593 product ions included *m/z* 575, 565 and the principal peak at 533; examination of products of the *m/z* 533 ion revealed fragments at *m/z* 504, 489, 476, the principal peak at 461, and 433; examination of products of the *m/z* 461 ion revealed multiple peaks as shown. The latter included, in particular, *m/z* 382, 366, 342, 328, 251, 235, 224 and 210.

Examination of a perennial ryegrass silage extract by full scan mass spectrometric analysis on a tandem quadrupole instrument (ESI(+)-MS/MS) confirmed the principal high molecular weight component at *m/z* 593, along with a "companion" fragment at *m/z* 609 (Figure 4). The principal extract component was identified at *m/z* 183, seen on this instrument owing to a greater practical sensitivity in the lower molecular weight range. Measurement of isotopic relative abundances for *m/z* 593 confirmed values seen by ESI(+)-ion trap MS (Figure 2), with M+1 = 37% and M+2 = 10%. The *m/z* 609 peak gives relatively similar M+1 at 38%, but a significantly higher M+2 at 25%.

Mass spectral analysis: evidence for alkali metal adducts

Our group has been successful in identifying adducts of organic compounds, including drug conjugates

© 2011 Informa Healthcare USA, Inc.

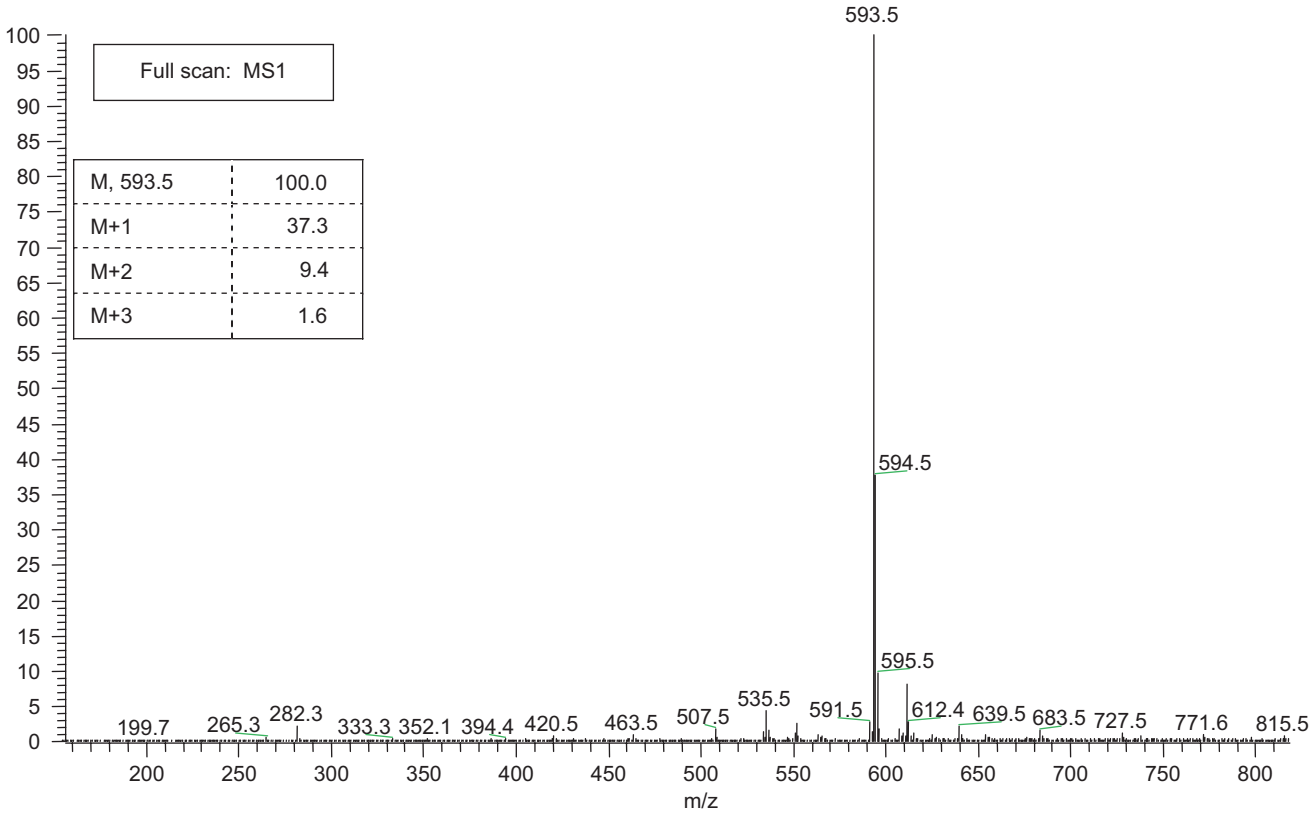

Figure 2. Full scan ESI(+) ion trap MS of isolated putative ergot-related compound at ~ 5-min retention time. Scans were acquired from *m/z* 150–2000 and full scale abundance (y-axis) was 1.19×10^7 intensity. The inset shows the relative abundances of M+1, +2 and +3 isotopes relative to the principal *m/z* 593.5 compound.

(Bosken et al., 2000) and macrocyclic lactones (Lehner et al., 2009). Verification of such complexes can involve titration with H^+, Li^+ or NH_4^+, or with other alkali metals (Bosken et al., 2000), self-consistent interpretations of related compounds (Lehner et al., 2009) and/or product ion scans (see below), or direct observation of Na^+ or K^+ ions, *m/z* 23 and 39, respectively (Lehner et al., 2009). We chose the latter two approaches for the work presented here.

Examination of the *m/z* 183 component seen in Figure 4 provided the product ion spectrum in Figure 5. The *m/z* 39 peak seen in this spectrum suggests potassium adduct formation. Making the simple subtraction *m/z* 183 – 39 = 144 and scanning the searchable version of the Merck Index for this molecular weight principally revealed the low molecular weight organic acid caprylic acid (octanoic acid) as a strong possibility, along with its isomers including ethyl caproate and valproic acid as alternative candidates. Principal peaks *m/z* 115, 101 and 65 agree ± 1 amu with the Wiley published electron impact mass spectrum of potassium-free octanoic acid. The presence of caprylic acid would not be unexpected, owing to its use as a fermentation stimulant and silage preservative (Abel et al., 2002).

Knowledge of the presence of alkali metal adducts aided in interpretation of the principal components of interest at *m/z* 539 and 609. Product ion scans of these ions as shown in Figure 6 revealed the presence of sodium (*m/z* 23) and potassium (*m/z* 39), respectively. Since both 539 – 23 and 609 – 39 give the same value of 570, this strongly suggested that these components are related and involve an uncharged molecular weight of 570. Table 1 lists components seen by ESI(+)MS/MS and examined by daughter ion analysis. *M/z* 183, 593 and 609 were the principal components seen to contain alkali metal components, and the resultant inferred molecular weights are tabulated.

Mass spectral analysis of the new compound as a sodium adduct

Table 2 lists mass spectral fragments seen as a result of ESI(+)-ion trap MS in comparison to those seen by ESI(+)MS/MS, both for the *m/z* 593 species as well as for the likely related *m/z* 609 component. Values calculated as arising by subtraction of the sodium (mass 23) or potassium (mass 39) components are shown in the shaded areas, and these calculations provide excellent evidence of unity between these disparate measurements, as seen specifically in the *m/z* 593 derived fragments (*m/z* 593, 565, 533, 476, 461, 433) from the two different instruments; in the observed fragments *m/z* 565, 489, 95, 81 and 60 seen on comparison of *m/z* 593 and 609 derived fragments from ESI (+)-MS/MS; and as seen by alkali metal subtracted fragments (*m/z* 526, 492, 482, 450, 438, 424, 382, 235, 197) on comparison of all three.

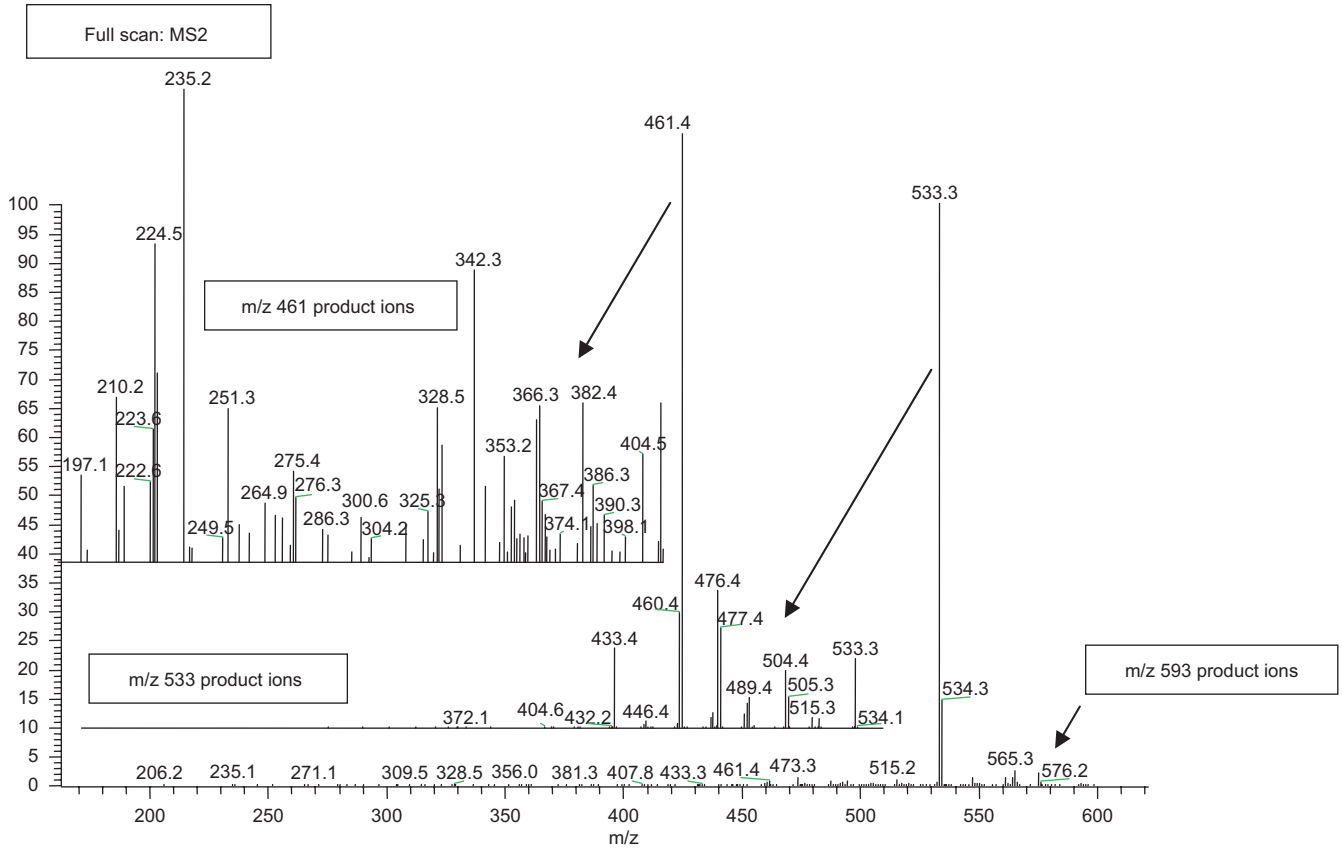

Figure 3. ESI(+) ion trap MS^n of isolated putative ergot-related compound at ~ 5.0-min retention time. Scans were acquired from *m/z* 150–600. Successive MS^n provided *m/z* 593 product ions (lowest scale), *m/z* 533 product ions (nested scale) and *m/z* 461 product ions (innermost nested scale) as labeled.

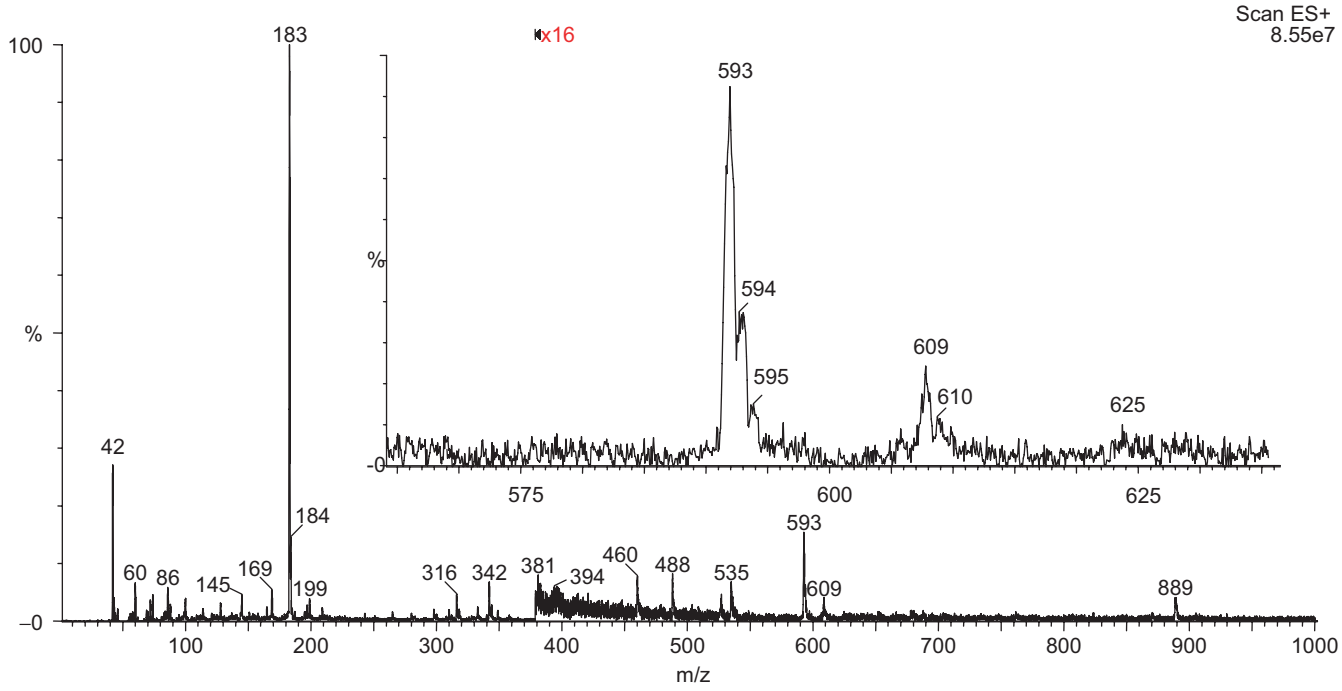

Figure 4. ESI(+)MS analysis of a silage sample diluted in 0.05% formic acid (aq):ACN, 1:1 and examined by direct infusion at 1.0 mL/h. Full scan spectrum was obtained through a combination of 38 sequential scans and background subtraction. Note enhancement (16-fold) of *m/z* 380–1000 region. The inset spectrum shows a blow up of *m/z* 565–635 region. Relative intensities for *m/z* 593 are 100, 37 and 10% for M, M+1 and M+2, respectively, and for *m/z* 609 they are 100, 38 and 25%.

© 2011 Informa Healthcare USA, Inc.

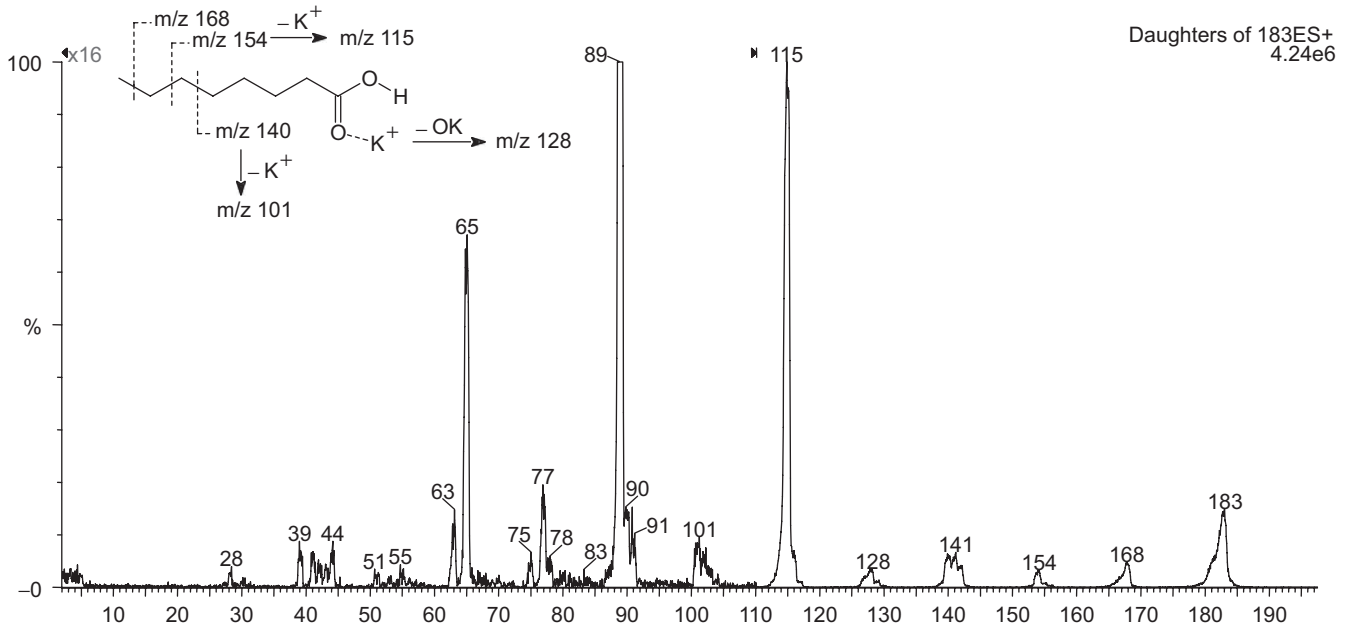

Figure 5. Product ion scan of *m/z* 183 seen in Figure 4. Note 16× enhancement of *m/z* 0–110 range. The inset shows an interpretation of the spectrum as arising from a caprylic acid-K^+ adduct, made likely by the presence of the *m/z* 39 potassium peak.

Mass spectral elucidation of the new peak structure

High resolution mass spectrometric instrumentation was unavailable for this work, so the following interpretations should be considered preliminary. Note, however, that our labs have had reasonable success in interpreting mass spectral fragments from low resolution, e.g. quadrupole, instruments, including data on isotopic abundances (Lehner et al., 2004a, 2004b, 2009).

General ergot alkaloid structures are summarized in Figure 7. Our earlier work discerned certain recurring mass spectral fragmentation motifs in the ergot alkaloids (Lehner et al., 2004a, 2005), enabling us to predict structures of new compounds. Specifically, we had considerable success in assigning structures to numerous unique or newly discovered ergopeptine alkaloids by unique recombination of amino acid R-groups already known to be incorporated into ergopeptines (Lehner et al., 2005). We decided to reapply this method as an initial approach and consider all possible genetic code-encoded amino acids plus ethyl as possible origins of R-groups in ergopeptines (R_1 and R_2 in structure C, Figure 7). Values of interest based on this type of calculation are listed in Table 3. None of the combinations directly provided m.w. 570, but even mws 574 (intact alkaloid) or 572 (dehydrate) could be considered as starting points for structure elucidation. Figure 8 shows an example of a putative ergot structure derived from application of reasoning with amino acid R-groups, in this case a lys/val structure making it an analog of the known ergot alkaloid ergovaline. However, although this approach may be capable of deriving unique candidates capable of fulfilling the expected 570 m.w. target, it suffers from two major drawbacks: (i) lack of precedent for such unusual R-groups in ergopeptines, and (ii) lack of "diagnostic" mass spectral fragments reflective of ergopeptine-related compounds, as summarized by Lehner et al. (2004a) and including values such as *m/z* 208 and 223, or 210 and 225 for those involving saturation of the 9,10-bond. This lack of diagnostic fragments was supported by parent ion scans for these ions in the silage derived material which revealed no candidate high m.w. components (data not shown).

We thus took several new approaches to deciphering the structure of the unique 570 m.w. compound, including (i) comparison of molecular weight and mass spectrometric fragments to a comprehensive mycotoxin database; (ii) comparison to a comprehensive ergot alkaloid database; (iii) mass spectrometric fragment analysis; and (iv) consideration of other chemical and spectral properties.

The clinical situation strongly suggested that the high molecular weight component of m.w. 570 is a unique ergot alkaloid, particularly since no other candidate ergot alkaloids were identifiable. The uniqueness of this compound was verified by reference to a comprehensive mycotoxin/fungal metabolite database (Nielsen & Smedsgaard, 2003); no entries in that 474-compound database provided relevant compounds in the 569–571 m.w. range, nor did any mass spectral data entries disclose ESI(+)MS fragments *m/z* 593, 533, 461 or 235 (i.e. principal fragments in Figure 3) in any manner that seemed to reflect on the discovery reported here.

We next scanned the ergot-specific database of Flieger and coworkers (Flieger et al., 1997). The best known ergot alkaloid skeletal structures including 6,7-secoergoline, ergoline, ergopeptine and ergopeptam basic skeletons are

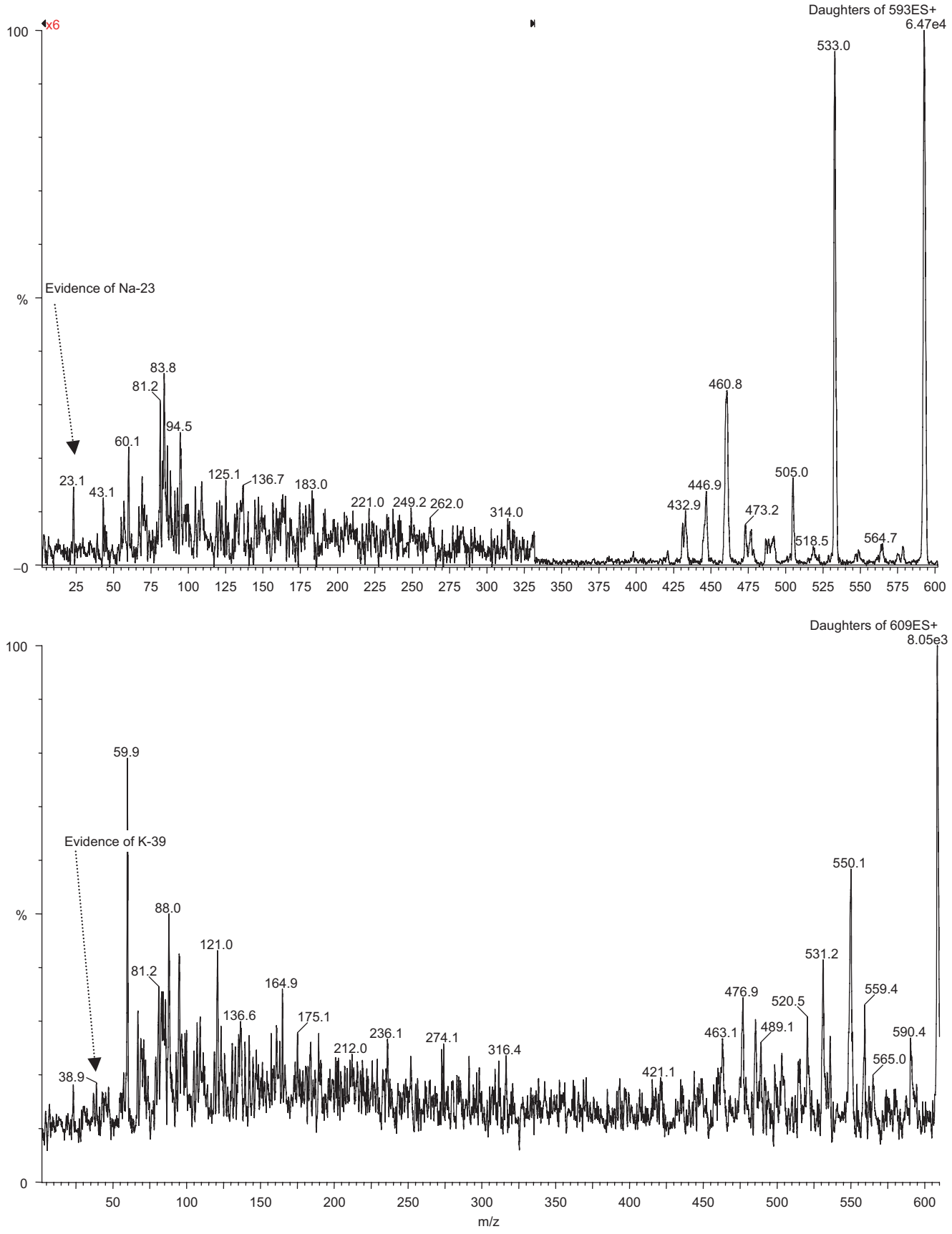

Figure 6. Product ion analysis of a silage sample for *m/z* 593 (top) and *m/z* 609 (bottom); note enhancement (×6) for *m/z* 20–325 region in the *m/z* 593 spectrum (top). Spectra were acquired as in Figure 4.

© 2011 Informa Healthcare USA, Inc.

Table 1. ESI(+)MS/MS analysis: revelation of Na^+ or K^+ adducts by examination of daughter ion spectra and inspection for *m/z* 23 or 39 fragments, respectively.

Molecular ion	Na/K evident	Likely m.w.
183	K	144
316	None	315
342	None	341
460	None	459
488	None	487
535	None	534
593	Na	570
609	K	570
889	Not examined	888 or 866

summarized in Figure 7. All possible known ergot alkaloid structures that could be condensed from this review are summarized in Table 4. The shaded section of Table 4 indicates the region of high molecular weight ergot alkaloid structures, including hypothetical demethylated or dehydrated variants. The closest possibilities wound up being fructofuranosyl-(2-1)-O-beta-D-fructofuranoside derivatives of 6,7-secoergoline derived from *Claviceps fusiformis* and their demethylated analogs, labeled W, X, Y and Z in Table 4. An example of such a structure, after Flieger et al. (1990) is shown in Figure 9. As a first approximation, for example, the hypothetical demethylated 566 m.w. variant X of the 580 m.w. starting compound Z would require reduction of two double bonds to give 570 m.w., shown as the first candidate structure A in Figure 10.

We believe that the difructosyl structures at 578 and 580 m.w. (Y and Z in Table 4) provide a valuable clue in that they are the only even m.w. compounds in the shaded high m.w. range of Table 4. With the exception of quaternary amines, the nitrogen rule of organic chemistry requires that compounds comprised of C,N,O,S,F,Cl, and Br have even molecular weights if the N-number is even (including zero) and odd m.w. if the N-number is odd (McLafferty & Turecek, 1993). Analogs of structures Y or Z therefore have the advantage of being of sufficiently high molecular weight without introducing an odd number of N-atoms as in the ergopeptines and ergopeptams.

The compounds of Table 4 comprise the atoms C, H, N, S and O, with a single entry at 593 m.w. offering an S atom. Consideration of the likelihood that the unique 570 m.w. species comprises only C, H, N and O atoms is supported by the lack of significant M+2 values in the relative isotopic contributions for *m/z* 593, ruling out possible S, P or halide functionalities, although S becomes a special consideration as discussed below. The relatively high M+2 for *m/z* 609 is not unexpected, owing to the considerable M+2 contribution of 7% for potassium, in contrast to lack of isotopic contributions from sodium. In any case, calculation of all possible molecular formulae with constraints as imposed according to the materials and methods for the Formula Calculator yielded 493 entries with m.w. 570 ± 0.5 and provided a range of M+1 isotopic contributions from 32 to 42%.

Structure A in Figure 10 meets the self-imposed stipulations of tight M+1 and M+2 isotopic contributions and therefore comparability to the mass spectrometric data. It is therefore a possible structure for the putative m.w. 570 ergot alkaloid similar to frucofuranosylated chanoclavine compounds seen in *C. fusiformis* (Flieger et al., 1997).

Mass spectrometric fragment analysis was the next step in dissecting the structure of the unique ergot alkaloid. Loss of 60 amu as in *m/z* 593→533 (Figure 3 and Figure 6, top) is suggestive of acetylation, with loss of neutral acetic acid as an explanation for the 60 loss, and a review of acetylated electron impact mass spectra reveals the loss of 60 as a predictable feature, e.g. 4,4-dimethyl-cholest-7-en-3-ol, 3-beta-acetate (NIST98 Library of EI-mass spectra). There is precedent for acetylation in fumigaclavine A from *Aspergillus fumigatus* and its isomer roquefortine A from *Penicillium roquefortii* (Flieger et al., 1997), but these are only m.w. 298 in Table 4. Fumigaclavine C adds an additional isoprenoid R-group (+68) but still falls far short at m.w. 366.

Supportive of a fructofuranosyl-(2-1)-O-beta-D-fructofuranoside ergot alkaloid is the alternative possibility that loss of 60 amu may occur as CH(OH)-CH(OH) fragments from fructosyl structures. Review of NIST98 EI-mass spectra shows the *m/z* 60 fragment in 1-O-methyl-D-fructose, for example. In addition, the 1,3,4,5,6-pentakis-O-(trimethylsilyl) derivative of D-fructose contains the significant *m/z* 204 consisting of the bis(trimethylsilyl) derivative of the CH(OH)-CH(OH) fragment further indicating the likelihood of such a fragmentation.

The spectral property of fluorescence enabled initial detection of the new unique ergot alkaloid and must be taken into consideration. Although there is no specific program by which fluorescence can be precisely predicted, structural motifs associated with fluorescence have nonetheless long been known. Several generalizations as to the structural requirements for fluorescence in solution include (i) an aromatic nucleus substituted by at least 1 electron-donating group, and (ii) a conjugated unsaturated system capable of a high degree of resonance (Duggan et al., 1957). The lysergic, i.e. unsaturated ergoline, ring system of ergots is generally accepted as the source of fluorescence in ergopeptines, and saturation of the 9,10 double bond eliminates fluorescence (Gyenes & Szasz, 1955; Wichlinski & Trzebinski, 1963; Mago-Karacsony et al., 1979). Although the Figure 10A candidate structure fulfills molecular weight and isotopic contribution requirements as well as deriving from literature precedents, it unfortunately carries the signal disadvantage of eliminating any double bond conjugation with the aromatic ring, thereby simultaneously eliminating chances for fluorescence. The alternative structure in Figure 10B allows reintroduction of the indole double bond, simply by eliminating a methyl group and substituting with a hydroxyl to maintain

Table 2. Summary of mass spectral fragment ion *m/z* values for the unknown ~5.0-min RT peak, with comparison of Oregon State University (ESI(+)-ion trap MS) and University of Kentucky (ESI(+)-MS/MS) data, arranged in order of decreasing size.

ESI(+) ion trap MS		ESI(+) MS/MS			
Calculated fragment 593 dau – Na	593 etc. dau[1]	593 dau	Calculated fragment 593 dau – Na	Calculated fragment 609 dau – K	609 dau
	593	593			609
570			570	570	
553	*576*	*577*	*554*	*551*	590
	565	565			565
542			542		559
		549	526	526	*550*
	533	533			531
		519		*520*	521
510			510	*511*	
	504	*505*	496		
		492		492	
	489				489
481			482	482	487
466	476	476	469		*477*
453		473	453		
			450	450	
				448	
	461	461			463
438		447	438	438	
437	460		424	424	
	433	433			421
410	*411*		410		
	404				
388					
381	382			382	
359	366			277	316
343	*342*				
319	328				
305	*275*				*274*
252	*251*				
228	235			235	*236*
212	210				
187	197			197	
174					*175*
				136	165
				126	121
		95			95
		84			88
		81	72	*82*	81
		60	*61*	56	60
			58	49	
		43	37	*42*	
		23	*20*	*21*	39

Small boxes show direct comparability between *m/z* 593 daughter ion fragments seen on the different instruments. Underlined bold values indicate direct comparability between observed values (*m/z* 593 dau and *m/z* 609 dau) or calculated values (*m/z* 593– Na [23] or *m/z* 609– K [39]) elsewhere in the table; italics indicate comparability between observed and calculated values differing by only ±1 amu. Calculated values are shown in the shaded areas.

[1]This column combines MS and MS^n data from Figure 3 for *m/z* 593, 533 and 461 daughter ion spectra.

the target 570 m.w.; however, this is unlikely sufficient for fluorescence, and the resulting molecular formula C_{26} H_{38} N_2 O_{12} has disadvantageous M+1/M+2 isotopic contributions, limiting the usefulness of candidate B in Figure 10.

Additional candidates C and D (Figure 10) were constructed by further modifications of the secoergoline side chain, i.e. by introduction of the additional double bond for assurance of fluorescence and the simultaneous removal of a methylene group for achievement of

© 2011 Informa Healthcare USA, Inc.

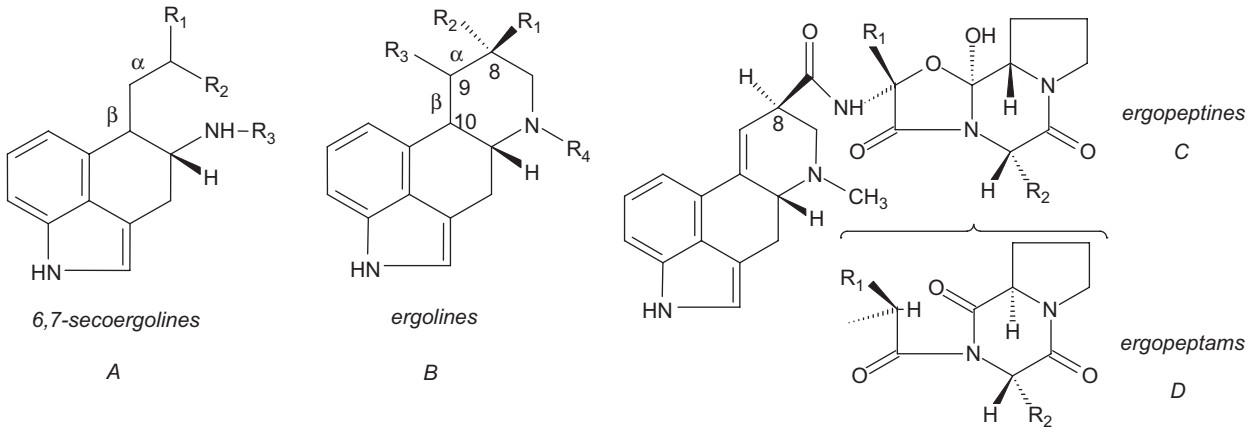

Figure 7. General ergot alkaloid structures, condensed from Flieger et al. (1997), including 6,7-secoergolines (A), ergolines (B), and lysergine derivatives ergopeptines (C) and ergopeptams (D). R-group components are discussed in the text and in Table 4.

Table 3. Hypothetical ergopeptine substituents from consideration of 20 amino acid R-groups plus ethyl as possibilities; shaded areas indicate values surrounding m.w. 570 both for calculated m.w.'s as well as for dehydrates.

2′ [or 5′] substituent	5′ [or 2′] substituent	Calculated m.w.	Dehydrate m.w.
phe	gly	567	549
cys	thr	567	549
cys	cys	569	551
His	ala	571	553
pro	leu/ileu	574	556
His	ethyl	585	567
His	ser	587	569
Leu/ileu	leu/ileu	589	571
Gln	pro	589	571
Lys	pro	589	571
Arg	ala	590	572
Gln	val	590	572
Lys	val	590	572
Asn	leu/ileu	590	572
Glu	pro	590	572
Glu	val	591	573
asp	leu/ileu	591	573
asn	asn	591	573

the target 570 m.w. Candidate C required an additional hydroxyl group to meet the target 570 m.w., whereas candidate D replaces the added hydroxyls with a single thiol group. Ironically, in order to accommodate a fluorescent structure (Figures 10C or D), the sought after agreement on isotopic abundances must be circumvented.

Therefore, in summary, the Figure 10D structure may at this time be the most satisfying possibility as it (i) takes advantage of the high m.w. fructofuranosyl group without introducing an odd number of N-atoms; (ii) does not require invocation of unusual amino acid substitution into an ergopeptine structure; (iii) derives the basis of its high molecular weight structure from model compounds in the literature; and (iv) most importantly, it introduces the double bonds at positions 2,3 and 9,10 most crucial for fluorescence in the molecule.

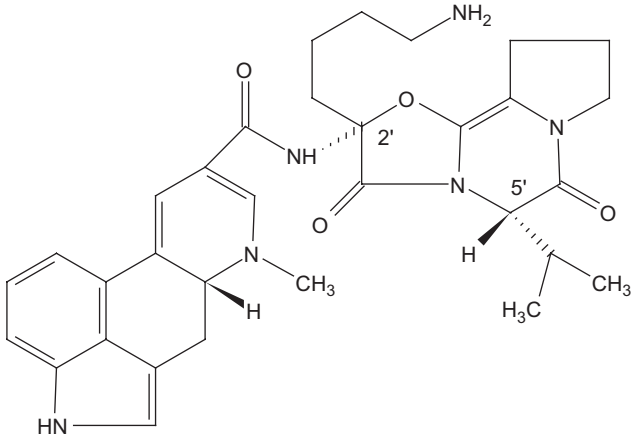

Figure 8. An example of an unusual ergopeptine structure of 570 m.w. related to ergovaline by substitution of its 5′-methyl group with a lysine R-group, by dehydration of the peptide ring system, and by introduction of an additional double bond into the lysergic ring system at position 8.

Discussion

The unique 5.0-min RT compound is suggested to be an ergot alkaloid-related compound by virtue of its association with clinical ergot-related symptomologies, its extractability with Ergosil, its detectability with a fluorescence detector ($\lambda_{ex}=250$; $\lambda_{em}=420$), and its chromatographic retention in the region between ergovaline (mw = 533) and ergotamine (mw = 581). Its apparent molecular weight is 570 owing to the predominance of the *m/z* 593.5 ion in the full scan ESI(+)MS (Figure 2) and its deduced tendency to complex with Na^+ or K^+ ions. We have done our best to offer structural rationales for this compound (Figures 8 and 10) and next discuss the evidence, supportive or otherwise, for each structure.

The stimulus for substituting alternative amino acid R-groups into the basic ergopeptine ring system (Table 3) derived from earlier successes in interpreting new or novel ergotoxins (Lehner et al., 2004a, 2005). Those were principally performed with recombinations of the known 2′-substituents of alanine, alpha-aminobutyrate

Table 4. Ergot alkaloid structure and molecular weight survey, based on basic structures in Figure 7 and including options for dehydrates and demethylated analogs where possible. Certain unusual structures were excluded, including paspaclavine, cycloclavine, aurantioclavine, clavicipitic acid, rugulovasine A and B and their chloro-derivatives, 4-dimethylallyltryptophan and its N-methyl derivative and epoxyagroclavine (Flieger, et al., 1997).

R_1	R_2	R_3	R_4	DB	Str	Isomers	MW	dehydrate	demethyl
CH_3	n.a.	H	CH_3	α	B	1	238		224
CH_3	H	H	CH_3	β	B		238		224
CH_3	CH_3	CH_3		α	A		240		226
CH_3	OH	H	H	β	B		240	222	226
CH_3	H	H	CH_3	none	B		240		226
CH_2OH	CH_3	H		α	A		242	224	228
CH_2OH	H	CH_3		none	A	2	244	226	230
CHO	CH_3	CH_3		α	A		254		240
$C(CH_3)=CH_2$	H	CH_3		none	A		254		240
CH_2OH	n.a.	H	CH_3	α	B		254	236	240
CH_2OH	H	H	CH_3	β	B		254	236	240
CH_3	OH	H	CH_3	β	B		254	236	240
CH_2OH	CH_3	CH_3		α	A	2	256	238	242
CH_3	OH	H	CH_3	none	B		256		242
CH_2OH	H	H	CH_3	none	B		256	238	242
H	CH_3	OH	CH_3	none	B	3	256	238	242
CH_3	H	OH	CH_3	none	B		256	238	242
$CONH_2$	H	H	CH_3	β	B	2	267		253
COOH	H	H	CH_3	β	B	2	268		254
COOH	H	H	CH_3	β	B		268		254
COOH	CH_3	CH_3		α	A		270		256
CH_2OH	n.a.	OH	CH_3	α	B		270	252	256
CH_2OH	OH	H	CH_3	β	B		270	252	256
$CONH_2$	OH	H	CH_3	β	B	2	283		269
$CONH_2$	OH	H	CH_3	β	B	1	283		269
H	CH_3	O(C=O) CH_3	CH_3	none	B		298		284
$CONHCH(CH_3)OH$	H	H	CH_3	β	B	2	311	293	297
$CONHCH(CH_3)CH_2OH$	H	H	CH_3	β	B	2	325	307	311
$CONHCH[CH(CH_3)_2]$ $COOCH_3$	H	H	CH_3	β	B		381		367
$CH_2O(C_6H_{10}O_4)OH$	n.a.	H	CH_3	α	B		416	398	402
$CH_2O(C_6H_{10}O_4)OH$	CH_3	CH_3		α	A		418	400	404
CH_3	CH_2CH_3				D		503	485	489
CH_3	$CH(CH_3)_2$				D		517	499	503
CH_2CH_3	CH_2CH_3				D		517	499	503
CH_3	CH_2CH_3				C		519	501	505
CH_3	$CH_2CH(CH_3)_2$				D		531	513	517
CH_3	$CH(CH_3)CH_2CH_3$				D		531	513	517
CH_2CH_3	$CH(CH_3)_2$				D		531	513	517
$CH(CH_3)_2$	CH_2CH_3				D		531	513	517
CH_3	$CH(CH_3)_2$				C		533	515	519
CH_2CH_3	CH_2CH_3				C		533	515	519
CH_2CH_3	$CH_2CH(CH_3)_2$				D		545	527	531
CH_2CH_3	$CH(CH_3)CH_2CH_3$				D		545	527	531
$CH(CH_3)_2$	$CH(CH_3)_2$				D		545	527	531
CH_3	$CH_2CH(CH_3)_2$				C		547	529	533
CH_3	$CH(CH_3)CH_2CH_3$				C		547	529	533

Table 4. continued on next page

© 2011 Informa Healthcare USA, Inc.

Table 4. Continued.

R_1	R_2	R_3	R_4	DB	Str	Isomers	MW	dehydrate	demethyl
CH_2CH_3	$CH(CH_3)_2$				C		547	529	533
$CH(CH_3)_2$	CH_2CH_3				C		547	529	533
$CH(CH_3)_2$	$CH_2CH(CH_3)_2$				D		559	541	545
$CH(CH_3)_2$	$CH(CH_3)CH_2CH_3$				D		559	541	545
CH_2CH_3	$CH_2CH(CH_3)_2$				C		561	543	547
CH_2CH_3	$CH(CH_3)CH_2CH_3$				C		561	543	547
$CH(CH_3)_2$	$CH(CH_3)_2$				C		561	543	547
CH_3	$CH_2C_6H_5$				D		565	547	551
$CH(CH_3)_2$	$CH_2CH(CH_3)_2$				C		575	557	561
$CH(CH_3)_2$	$CH(CH_3)CH_2CH_3$				C		575	557	561
$CH(CH_3)_2$	$CH(CH_3)CH_2CH_3$				C		575	557	561
$CH(CH_3)_2$	$CH_2CH(CH_3)_2$				C		575	557	561
$CH_2O(C_6H_{10}O_4)O(C_6H_{10}O_4)OH$	n.a.	H	CH_3	α	B		578 [Y]	560	564 [W]
CH_2CH_3	$CH_2C_6H_5$				D		579	561	565
$CH_2O(C_6H_{10}O_4)O(C_6H_{10}O_4)OH$	CH_3	CH_3		α	A		580 [Z]	562	566 [X]
CH_3	$CH_2C_6H_5$				C		581	563	567
$CH(CH_3)_2$	$CH_2CH_2CH(CH_3)_2$				C		589	589	575
$CH(CH_3)_2$	$(CH_2)_2SCH_3$				C		593	575	579
$CH(CH_3)_2$	$CH_2C_6H_5$				D		593	575	579
CH_2CH_3	$CH_2C_6H_5$				C		595	577	581
$CH(CH_3)_2$	$CH_2C_6H_5$				C		609	591	595

n.a., not applicable; DB, # additional double bonds. (cf. Figure 7); str, structure A–D in Figure 7.
Compounds arranged in order of increasing molecular weight. Boxed, shaded section refers to m.w. range of interest in defining unknown 5-min RT compound.
[1]C_{10}-H in beta position; [2]$R_1 \leftrightarrow R_2$ isomer; [3]+ R_3 stereoisomer.

and valine with the known 5′-substituents valine, phenylalanine, isoleucine or leucine. However, unusual recombinations within this limited subset did not allow satisfactory accommodation of the 570 m.w., particularly its even value. Consideration of the twenty major genetic code-encoded amino acids was particularly driven by the need to introduce nitrogenous R-group containing amino acids such as lysine to provide an even N-number. This consideration is not necessarily unlikely since new amino acids have been discovered in ergot alkaloid structures, including methionine and norleucine (Cvak et al., 1996, 2005), although apparently not yet the required lysine, asparagine, tryptophan or glutamine, each capable of introducing a single N-atom, or arginine capable of introducing three N-atoms. The most acceptable posited ergopeptine structure starts with an m.w. of 572 in Table 3 and would include dehydrated 2′-ala/5′-arg, 2′-val/5′gln, 2′-val/5′-lys, 2′-gln/5′-val, 2′-lys/5′-val, 2′-asn/5′-leu or 2′-asn/5′-ile combinations since one of each combination is in the already known amino acid subset and would require only one unusual amino acid. In addition, another double bond or even a ring would then be required to reduce the m.w. by 2 hydrogen atoms. An example structure from this category derived from the 2′-lys/5′-val combination is illustrated in Figure 8. It is unknown whether this structure would explain the uncharacteristic fragmentation (Figures 3 and 6), although it is strongly suspected that it should provide *m/z* 221 and 206 fragments similar to *m/z* 223/208 fragments generally seen from ergots bearing intact ergoline ring systems (Lehner et al., 2004a, 2005).

The structurally different posited chanoclavine-fructosides (Figure 10) derive from previous work of other investigators (Flieger et al., 1997). The *C. fusiformis* strain W1 was found capable of considerable fructosylation ability toward chanoclavine; however, in order to accommodate the 570 m.w. in our work, demethylation and reduction of two double bonds was necessary. The advantage of such a structure is that it avoids the even molecular weight problem inherent in the ergopeptines; it provides sufficiently high mass by incorporation of the fructofuranosyl-(2,1)-O-beta-D-fructofuranoside group; and it provides at least a possible explanation for the uncharacteristic fragmentation pattern of this compound by positing a secoergoline ring system. Fungal databases at the USDA Agricultural Research Service (http://nt.ars-grin.gov) indicate reported *Claviceps* infection of cenchrus, panicrum, pennisetum and sorghum species, thereby providing a possible pretext for infection of forage grasses or grains. Unfortunately, the structure as shown in Figure 10A changes the level of double bond conjugation in the lysergic ring system, which would likely dramatically change its fluorescence characteristics, in turn, and make it undetectable by this methodology. In addition, it

would have been reassuring to find a mono-fructosyl version of this compound akin to the findings of Flieger et al. (1990); unfortunately, no Na-complexed compounds of *m/z* 431 or H-complexed compounds of *m/z* 409 were identified (Figures 2 & 4), at least not within the purified 5-min peak fraction.

Another consideration is that the MS^3 spectrum in Figure 3, shown as product ions of *m/z* 461, includes *m/z* 225 and 210. This is similar to product ions predicted for ergopeptine alkaloids hydrogenated in the 6,7-position such as dihydroergocornine and dihydroergocristine (Lehner et al., 2004a). Although we generally dismiss the intact ergoline ring structures of Figure 7 (B, C and D) in favor of the secoergolines owing to the precedent of fructofuranosyl structures in the literature (Flieger et al., 1997), we must at the same time acknowledge that the effects of sodium adduction on fragmentation patterns can be somewhat unpredictable. Therefore, the intact ergoline ring compounds are not fully excluded; however, compounds with dihydrogenated ergoline ring structures, whether brought to the target mass of 570 by fructofuranosylation or not, must still encounter the problem of greatly diminished fluorescence owing to double bond hydrogenation.

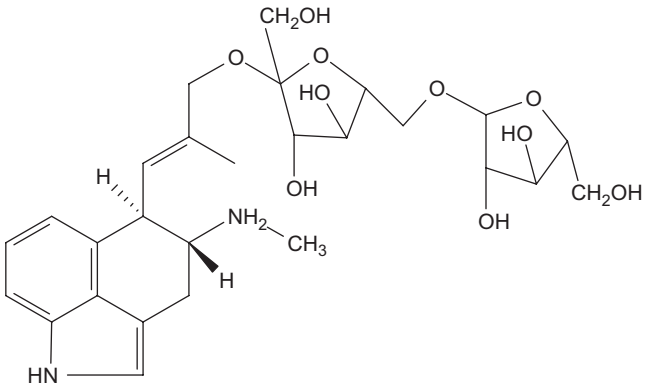

Figure 9. Example of a secoergoline derivative with a fructofuranoside side chain. This is specifically a chanoclavine derivative, Chem Abstracts name [4R-[4α,5β(E)]]-2-methyl-3-[1,3,4,5-tetrahydro-4-(methylamino)benz[cd]indol-5-yl]-2-propenyl 1-O-β-D-fructofuranosyl-β-D-fructofuranoside, after Flieger et al. [26]. The compound is $C_{28}H_{40}N_2O_{11}$, 580 m.w.

In addition to possible *N. lolii* or *C. fusiformis* origins for the newly discovered compound described herein, we must consider the possibility that the compound of interest is a product of the silage fermentation process. Since perennial ryegrass has long been grown extensively in the Willamette Valley, bovine reproductive difficulties might have been expected to occur over time with greater frequency unless biochemical aspects of the historically more recent silage fermentation process were a requisite part of the toxin generation process. Such fermentation-dependent toxin generation processes

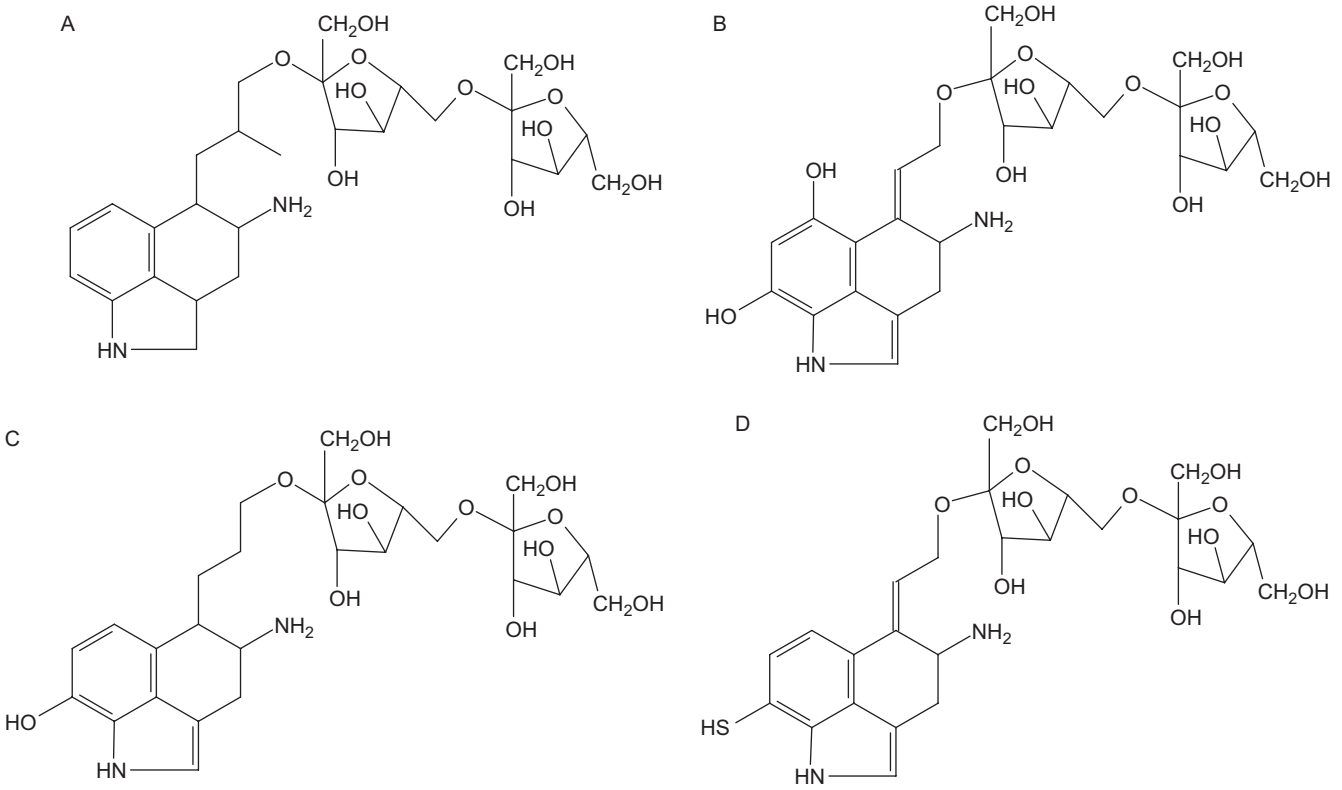

Figure 10. Candidate structures for the new ergot alkaloid, basically as fructofuranosyl derivatives of chanoclavine. A, $C_{27}H_{42}N_2O_{11}$, M+1 = 31.8%, M+2 = 7.0%, fulfills isotopic contributions determined for *m/z* 593; B, $C_{26}H_{38}N_2O_{12}$, M+1 = 30.7%, M+2 = 6.8%, hydroxylated, demethylated, dehydrogenated version of A, introducing at least one double bond for enhanced spectral properties; C, $C_{25}H_{34}N_2O_{13}$, M+1 = 29.6%, M+2 = 6.7%, modified version of B, introducing an additional double bond for enhanced spectral properties; D, $C_{25}H_{34}N_2O_{11}S_1$, M+1 = 30.3%, M+2 = 10.9%, replacement of hydroxyl groups of C with single thiol group.

© 2011 Informa Healthcare USA, Inc.

may occur through biochemical interactions between bacteria and fungal mycotoxins, as set forth by Cho et al. (2010), Meca et al. (2010) and Thibodeau et al. (2004), for example. Preliminary experiments suggest that the unfermented grasses alone do not contain the new presumed ergot alkaloid, although further experiments are required to demonstrate this definitively. Whether the compound is in fact a direct microbial byproduct or a fungal endophytic product metabolically induced or altered by fermentative microorganisms thus remains to be determined.

In conclusion, it is our hope that, despite the inherent difficulties of the proposed structures, they may provide useful conceptual starting points for eventual elucidation of this new presumed ergot alkaloid.

Declaration of interest

Funding for this project was provided in part by the Oregon Agricultural Experiment Station (project ORE00871) and the United States Department of Agriculture (USDA), Agricultural Research Service under cooperative agreement # 58–6227-8-044, Dale Bumpers Small Farms Research Center, Booneville AR. Any opinions, findings, conclusions, or recommendation expressed in this publication are those of the author(s) and do not necessarily reflect the view of the U.S. Department of Agriculture.

Published as paper #396 from the Equine Pharmacology, Therapeutics and Toxicology Program at the Maxwell H. Gluck Equine Research Center and Department of Veterinary Science, University of Kentucky. Published as Kentucky Agricultural Experimental Station Article # 11–14-031 with the approval of the Dean and Director, College of Agriculture and The Kentucky Agricultural Experimental Station. This work was supported in part by ongoing research support from The National Horsemen's Benevolent and Protective Association and the Alabama, Arizona, Arkansas, Canada, Charles Town (West Virginia), Florida, Iowa, Indiana, Kentucky, Louisiana, Michigan, Minnesota, Nebraska, Ohio, Oklahoma, Ontario (Canada), Oregon, Pennsylvania, Tampa Bay Downs (Florida), Texas, Washington State, and West Virginia Horsemen's Benevolent and Protective Associations and the Florida Horsemen's Charitable Foundation, the Oklahoma Quarter Horse Racing Association and the Neogen Corporation.

References

Abel H, Immig I, Harman E. (2002). Effect of adding caprylic and capric acid to grass on fermentation characteristics during ensiling and in the artificial rumen system RUSITEC. Animal Feed Science Technology 99:65–72.

Bernard J, Chestnut A, Erickson B, Kelly F. (1993). Effects of prepartum consumption of endophyte-infested tall fescue on serum prolactin and subsequent milk production of holstein cows. Journal of Dairy Science 76:1928–1933.

Blodgett DJ. (2001). Fescue toxicosis. Vet Clin North Am Equine Pract 17:567–577.

Bosken JM, Lehner AF, Hunsucker A, Harkins JD, Woods WE, Karpiesiuk W, Carter WG, Boyles J, Fisher M, Tobin T. (2000). Direct MS-MS identification of isoxsuprine-glucuronide in post-administration equine urine. Can J Vet Res 64:112–116.

Brown MA, Brown AH Jr, Jackson WG, Miesner JR. (1996). Milk production in Angus, Brahman, and reciprocal-cross cows grazing common bermuda grass or endophyte-infected tall fescue. J Anim Sci 74:2058–2066.

Browning R Jr. (2004). Effects of endophyte-infected tall fescue on indicators of thermal status and growth in Hereford and Senepol steers. J Anim Sci 82:634–643.

Browning R Jr, Schrick FN, Thompson FN, Wakefield T Jr. (1998). Reproductive hormonal responses to ergotamine and ergonovine in cows during the luteal phase of the estrous cycle. J Anim Sci 76:1448–1454.

Burke JM, Spiers DE, Kojima FN, Perry GA, Salfen BE, Wood SL, Patterson DJ, Smith MF, Lucy MC, Jackson WG, Piper EL. (2001). Interaction of endophyte-infected fescue and heat stress on ovarian function in the beef heifer. Biol Reprod 65:260–268.

Cheeke PR. (1998). Natural Toxicants in Feeds, Forages, and Poisonous Plants, Second Edition. Interstate Publishers, Inc.: Danville, Illinois.

Cho KJ, Kang JS, Cho WT, Lee CH, Ha JK, Song KB. (2010). *In vitro* degradation of zearalenone by *Bacillus subtilis*. Biotechnol Lett 32:1921–1924.

Cole JR Jr, Sulzer CR, Pursell AR. (1973). Improved microtechnique for the leptospiral microscopic agglutination test. Appl Microbiol 25:976–980.

Cottral G. (1978). Manual of standardized methods for veterinary microbiology. Cornell University Press: Ithaca, New York.

Craig AM, Bilich D, Hovermale JT, Welty RE. (1994). Improved extraction and HPLC methods for ergovaline from plant material and rumen fluid. J Vet Diagn Invest 6:348–352.

Cvak L, Jegorov A, Sedmera P, Císarová I, Cejka J, Kratochvíl B, Pakhomova S. (2005). Norleucine, a natural occurrence in a novel ergot alkaloid gamma-ergokryptinine. Amino Acids 29:145–150.

Cvak L, Minar J, Pakhomova S, Ondracek J, Kratochvil B, Sedmera P, Havlicek V, Jegorov A. (1996). Ergoladinine, an ergot alkaloid. Phytochemistry 42:231–233.

Dalziel JE, Finch SC, Dunlop J. (2005). The fungal neurotoxin lolitrem B inhibits the function of human large conductance calcium-activated potassium channels. Toxicol Lett 155:421–426.

Duggan DE, Bowman RL, Brodie BB, Udenfriend S. (1957). A spectrophotofluorometric study of compounds of biological interest. Arch Biochem Biophys 68:1–14.

Flieger M, Kren V, Zelenkova NF, Sedmera P, Novak J, Sajdl P. (1990). Ergot alkaloid glycosides from saprophytic cultures of *claviceps*, ii. Chanoclavine i fructosides. Journal of Natural Products 53:171–175.

Flieger M, Wurst M, Shelby R. (1997). Ergot alkaloids–sources, structures and analytical methods. Folia Microbiol (Praha) 42:3–29.

Gyenes I, Szasz K. (1955). The fluorimetric determination of ergot alkaloids. Magyar Kemiai Folyoirat 61:393–398.

Jackson JA, Sorgho Z, Hatton RH. (1988). Effect of nitrogen fertilization or urea addition and ensiling as large round bales of endophyte infected tall fescue on fescue toxicosis when fed to dairy calves. Nutrition Reports International 37:335–345.

Joost RE. 1995. Acremonium in fescue and ryegrass: Boon or bane? A review. J Anim Sci 73:881–888.

Kim J, Kim C, Ahn G, Park E, Kim C, Park K. (2007). Ergovaline levels in tall fescue and its effect on performance of lactating cows. Animal Feed Science and Technology 136:330–337.

Lean IJ. (2001). Association between feeding perennial ryegrass (*Lolium perenne* cultivar Grasslands impact) containing high concentrations of ergovaline, and health and productivity in a herd of lactating dairy cows. Aust Vet J 79:262–264.

Lehner AF, Craig M, Fannin N, Bush L, Tobin T. (2005). Electrospray[+] tandem quadrupole mass spectrometry in the elucidation of ergot alkaloids chromatographed by HPLC: Screening of grass

or forage samples for novel toxic compounds. J Mass Spectrom 40:1484–1502.

Lehner AF, Craig M, Fannin N, Bush L, Tobin T. (2004a). Fragmentation patterns of selected ergot alkaloids by electrospray ionization tandem quadrupole mass spectrometry. J Mass Spectrom 39:1275–1286.

Lehner AF, Horn J, Flesher JW. (2004b). Mass spectrometric analysis of 7-sulfoxymethyl-12-methylbenz[a]anthracene and related electrophilic polycyclic aromatic hydrocarbon metabolites. J Mass Spectrom 39:1366–1378.

Lehner AF, Petzinger E, Stewart J, Lang DG, Johnson MB, Harrison L, Seanor JW, Tobin T. (2009). ESI+ MS/MS confirmation of canine ivermectin toxicity. J Mass Spectrom 44:111–119.

Mago-Karacsony E, Balogh T, Lang T, Uskert E. (1979). Hydrogenation of ergolenes. Hung. Teljes, 25 pp. Patent 16821 19790728 written in Hungarian.

McLafferty FW, Turecek F. (1993). Interpretation of Mass Spectra, 4th Edn. Sausalito, CA: University Science Books.

Meca G, Sospedra I, Soriano JM, Ritieni A, Moretti A, Mañes J. (2010). Antibacterial effect of the bioactive compound beauvericin produced by *Fusarium proliferatum* on solid medium of wheat. Toxicon 56:349–354.

National Veterinary Services Laboratories (2001). Use of leptospira multivalent fluorescent antibody conjugate to detect leptospira in diagnostic specimens. Btypsop4008.01 in National Veterinary Services Laboratories testing protocol.

Nielsen KF, Smedsgaard J. (2003). Fungal metabolite screening: Database of 474 mycotoxins and fungal metabolites for dereplication by standardised liquid chromatography-UV-mass spectrometry methodology. J Chromatogr A 1002:111–136.

Oliver JW. (1997). Physiological manifestations of endophyte toxicosis in ruminant and laboratory species. Proceedings of the Third International Symposium on Acremonium/Grass Interactions: Athens Georgia, 311–346.

Oliver JW. (2005). Pathophysiologic response to endophyte toxins in Neotyphodium in cool-season grasses. Blackwell Publishing: Ames, Iowa, pp. 291–304.

Porter JK, Thompson FN Jr. (1992). Effects of fescue toxicosis on reproduction in livestock. J Anim Sci 70:1594–1603.

Roberts C, Kallenbach R, Hill N. (2002). Harvest and storage method affects ergot alkaloid concentration in tall fescue. Online. Crop Management DOI:10.1094/CM-2002-0917–1001-BR.

Rossi CR, Kiesel GK. (1971). Microtiter tests for detecting antibody in bovine serum to parainfluenza 3 virus, infectious bovine rhinotracheitis virus, and bovine virus diarrhea virus. Appl Microbiol 22:32–36.

Thibodeau MS, Poore MH, Hagler WM Jr, Rogers GM. (2004). Effect of fermentation on Sweetpotato (Ipomoea batatas) toxicity in mice. J Agric Food Chem 52:380–384.

Wichlinski L, Trzebinski J. (1963). Fluorometric method for the assay of impurities in hydrogenated ergot alkaloids. Acta Pol Pharm 20:31–34.

© 2011 Informa Healthcare USA, Inc.

Copyright of Toxicology Mechanisms & Methods is the property of Taylor & Francis Ltd and its content may not be copied or emailed to multiple sites or posted to a listserv without the copyright holder's express written permission. However, users may print, download, or email articles for individual use.